Journal of Photochemistry and Photobiology A: Chemistry 213 (2010) 23–29

Contents lists available at ScienceDirect

Journal of Photochemistry and Photobiology A: Chemistry

journal homepage: www.elsevier.com/locate/jphotochem

Synthesis and characterization of squaric acid based NIR dyes for their application towards dye-sensitized solar cells

Takafumi Inoue [a], Shyam S. Pandey [a,*], Naotaka Fujikawa [a], Yoshihiro Yamaguchi [b], Shuji Hayase [a]

[a] Kyushu Institute of Technology, 2-4 Hibikino, Wakamatsu, Kitakyushu, Japan
[b] Nippon Steel Chemical Company Limited, Nakabaru, Tobata, Kitakyushu, Japan

ARTICLE INFO

Article history:
Received 15 December 2009
Accepted 21 April 2010
Available online 29 April 2010

Keywords:
Dye sensitization
Solar cells
Aggregation
Squaraine dyes
CDCA
Nanocrystalline TiO_2

ABSTRACT

Synthesis of novel cyan-colored sensitizing dyes bearing squaric acid core and 2,3,3-trimethyl-indole as terminal moieties has been conducted in order to fabricate dye-sensitized solar cells based on nanoporous TiO_2. It has been found that position of –COOH functionality utilized for anchoring with TiO_2 surface has a marked effect on solar cell performance. Carboxylic acid group directly substituted to indole ring gave about 5-fold higher conversion efficiency as compared to the dye when it was substituted in alkyl chain of the indole ring. Efficiency has been found to be hampered due to aggregation and enhancement in the efficiency was observed when dyes were used with chenodeoxycholic acid (CDCA). Using CDCA and long alkyl substituent at the N-position of indole ring to prevent aggregation and enhanced TiO_2 surface passivation, respectively, has achieved a solar conversion efficiency of 3.15% with a short circuit current density of 7.26 mA/cm^2, an open circuit voltage of 0.64 V and a fill factor of 0.68 for **SQ-5** under standard AM 1.5 solar irradiation.

1. Introduction

Dye-sensitized solar cells (DSSCs) are one of the cheap alternatives to silicon solar cells for efficient harvesting of solar energy into electrical energy reaching photoconversion efficiency over 10% having efficient light absorption in the visible region of the solar spectrum [1,2]. Further enhancement in the conversion efficiency is possible by extending the absorption of sensitizing dyes in near infrared (NIR) regions. One of the most important and challenging factors attributed to the lower efficiency of the DSSCs as compared to silicon solar cells, is the lower optical absorption window (400–800 nm) of organic dyes which is smaller than the optical absorption window of crystalline silicon (500–1100 nm). A number of organic dyes giving high photoconversion efficiency similar to inorganic ruthenium based dyes have been reported but their lower optical absorption window offers stumbling block towards further increase in the conversion efficiency utilizing hybrid or tandem DSSC architecture [3,4]. In an attempt towards development of NIR organic dyes, Campbell et al. [5] have reported efficient porphyrin based sensitizers giving photoconversion efficiency between 5% and 7% having photon harvesting window less than 700 nm offers the hindrance for fabrication of hybrid DSSC with ruthenium based dyes for their further enhancement in the conversion efficiency. Recently, organic NIR sensitizing dyes bearing phthalocyanine and squaric acid core having photon harvesting beyond 700 nm have attracted a good deal of attention by material scientists owing to their potentiality towards utilization in the fabrication of tandem and hybrid DSSC [6–9].

Recently, Inakazu et al. have reported the extension of optical absorption window by selective adsorption of two dyes on nanoporous TiO_2 under pressurized CO_2 atmosphere leading to the enhancement in photoconversion efficiency [10]. Broadening in the light absorption in the extended wavelength region has also been reported using a mixture of organic dyes which do not create any hindrance with their sensitization properties [11]. It is believed that in dye cocktail two dyes are supposed to be arranged in a random distribution of dyes in the nanoporous TiO_2 layer. In an interesting report based on their investigation using confocal laser fluorescence microscope, Noma et al. have emphasized that it is possible to make a dye double layer hybrid DSSC using a dye cocktail by a judicious selection of two dyes under investigation leading to the light absorption in extended wavelength region [12]. Such studies have proved the potentiality of search for the more efficient sensitizers exhibiting light absorption in the near infrared wavelength region.

Owing to its higher stability, dyes based on squaric acid possessing a sharp and intense absorption band in the near infrared (NIR) region have attracted their attention towards application as sensi-

* Corresponding author at: Kyushu Institute of Technology, Graduate School of Life Science and Systems Engineering, 2-4 Hibikino, Wakamatsu, Kitakyushu, Fukuoka 808-0196, Japan. Tel.: +81 93 695 6044; fax: +81 93 695 6005.
E-mail address: shyam@life.kyutech.ac.jp (S.S. Pandey).

1010-6030/$ – see front matter © 2010 Elsevier B.V. All rights reserved.
doi:10.1016/j.jphotochem.2010.04.015

tizer in electrography, optical data storage and non-linear optical applications [13,14]. This class of dyes are able to sensitize the large band gap semiconductors leading to their application as sensitizer for photovoltaic applications, however, their lower efficiency of sensitization in DSSCs [15] need more logical dye design and synthesis. Das and co-workers [16] have demonstrated that unsymmetrical squaraine dyes shows better sensitization performance for DSSC as compared to their symmetrical dye counterpart led to the increased interest of material science community. Squaric acid based dyes are well known to form aggregates leading to decreased efficiency of sensitization resulting into decreased DSSC performance [17,18]. Present article deals with synthesis and application of some novel squaric acid dyes as sensitizer for the DSSC based on nanoporous TiO_2. An attempt has also been made to delineate the implication of structure of these novel sensitizers on photoconversion efficiency of DSSC based on such dyes.

2. Experimental

2.1. Materials, instruments and methods

All the chemicals for synthesis or solvents are of analytical or spectroscopic grade and used as received without further purification. Synthesized SQ-dyes and dye intermediates under investigation were analyzed by high performance liquid chromatography (JASCO) for purity, MALDI-TOF-mass/FAB-mass spectrometry in positive ion monitoring mode and nuclear magnetic resonance spectroscopy (NMR, 500 MHz) for structural elucidation. Electronic absorption spectroscopic investigations in solution and thin film adsorbed on TiO_2 surface was conducted using UV–visible spectrophotometer (JASCO model V550). Optimized geometries of final dyes along with the highest occupied molecular orbital (HOMO) and lowest unoccupied molecular orbital (LUMO) were calculated without any symmetry restriction at B3LYP/6-311G level of calculation using Gaussian 03 program package.

2.2. Synthesis of SQ-dyes and dye intermediates

Side chain carboxy functionalized indole derivative 1-(2-carboxyethyl)-2,3,3-trimethyl-3H-indolium iodide (**2a**) was synthesized following the method by Chen et al. [19] while aromatic ring carboxy functionalized indole derivative 2,3,3-trimethyl-3H-indole-5-carboxylic acid (**1b**) was synthesized following the methodology reported by Pham et al. [20]. Squaric acid based symmetrical squaraine dyes (**SQ-1**, **SQ-2**, **SQ-3**, **SQ-5**) and unsymmetrical squaraine dye (**SQ-4**) used in the present study have been synthesized following the methodology adopted by Oswald et al. [21] as shown in Schemes 1 and 2, respectively.

2.2.1. Synthesis of 1-(2-carboxyethyl)-2,3,3-trimethyl-3H-indolium iodide [2a]

In a round bottom flask fitted with condenser, 2,3,3-trimethyl-3H-indole (1.61 g; 10 mmol) and 3-iodopropanoic acid (4.0 g; 20 mmol) were added followed by 20 ml of 1,2-dichlorobenzene. Reaction mixture was heated at 110 °C for 16 h under N_2 atmosphere. Reaction progress was monitored by TLC and HPLC. Reaction mixture was cooled and then filtered. Precipitate was finally washed by ample ethyl acetate which finally gave 1.7 g of pinkish white titled compound in 48% yield. As confirmed by HPLC product purity was >98%, MALDI-TOF-mass (measured = 232.67, calculated = 232.13).

2.2.2. Synthesis of 2,3,3-trimethyl-3H-indolium-5-carboxylic acid [1b]

In a round bottom flask fitted with condenser and N_2 purging, 4-hydrazinobenzoic acid (5.0 g; 32.85 mmol), glacial acetic acid (80 ml), sodium acetate (5.5 g; 67 mmol) and 3-methyl-2-butanone (4.45 g; 51.5 mmol) were added. Reaction mixture was refluxed at 120 °C for 8 h leading to brown suspension. Acetic acid was evaporated followed by addition of 9:1 water methanol mixture on ice-bath leading to precipitation. Residue was filtered and dried giving 3.7 g of titled compound as off white powder in 56%

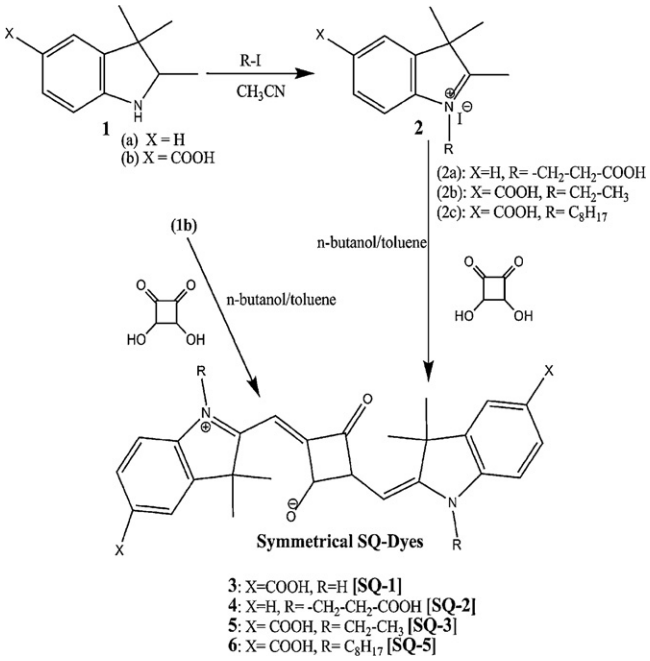

Scheme 1. Synthesis of symmetrical squaraine dyes.

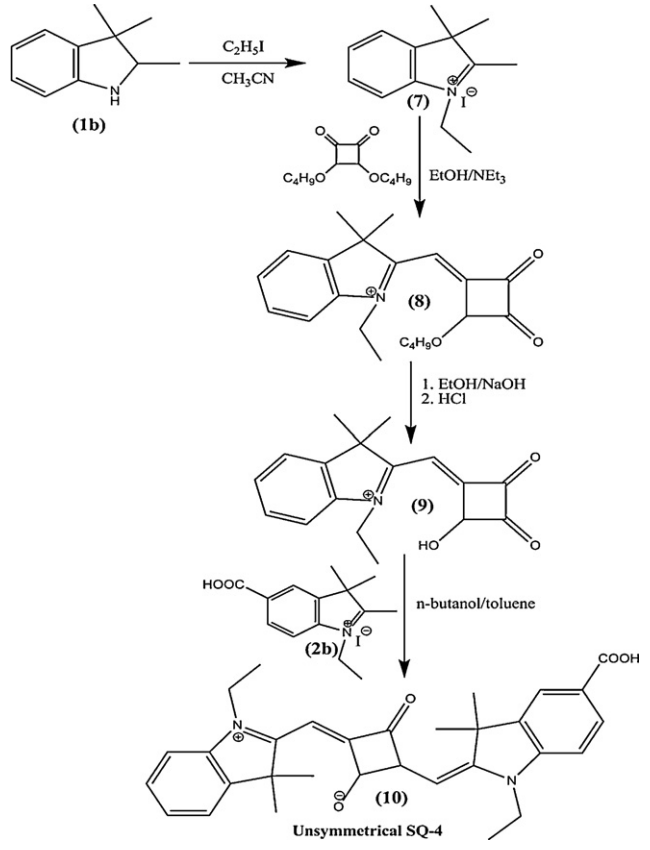

Scheme 2. Synthesis of unsymmetrical squaraine dye **SQ-4**.

yield. HPLC analysis of product suggests that compound was 100% pure. FAB-mass (measured 203, calculated 203.09) and ^{1}H NMR (500 MHz, $CDCl_3$): d/ppm = 7.99 (s, H-4), 7.93 (d, J = 9.0 Hz, H-6), 7.59 (d, H = 8.0 Hz, H-7), 2.23 (s, 3H, H-10), 1.28 (s, 6H, H-11+12) verifies the successful synthesis of the compound. For NMR chart see Supporting information S5.

*2.2.3. Synthesis of 5-carboxy-2,3,3-trimethyl-1-ethyl-3H-indolium iodide [**2b**]*

820 mg (4 mmol) of 2,3,3-trimethyl-3H-indole-5-carboxylic acid and 3.21 g (20 mmol) of 1-iodoethane were dissolved in 60 ml of dehydrated acetonitrile and reaction mixture was refluxed for 18 h under nitrogen. After completion of the reaction, solvent was evaporated and the crude product was washed with ample diethyl ether giving 1.14 g of titled compound as off white powder in 79% yield having 98% purity as confirmed by HPLC. FAB-mass (measured 232.0; calculated 232.13).

*2.2.4. Synthesis of 5-carboxy-2,3,3-trimethyl-1-octyl-3H-indolium iodide [**2c**]*

617 mg (3 mmol) of 2,3,3-trimethyl-3H-indole-5-carboxylic acid and 2.16 g (9 mmol) of 1-iodooctane were dissolved in 30 ml of dehydrated acetonitrile and reaction mixture was refluxed for 72 h under nitrogen. After completion of the reaction, solvent was evaporated and the crude product was washed with ample diethyl ether giving 956 mg (2.16 mmol) of titled compound as off white powder in 72% yield having 98% purity as confirmed by HPLC. FAB-mass (measured 316.0; calculated 316.23).

*2.2.5. Synthesis of 2,3,3-trimethyl-1-ethyl-3H-indolium iodide [**7**]*

3.17 g (20 mmol) of 2,3,3-trimethyl-3H-indole and 4.68 g (30 mmol) of 1-iodoethane were dissolved in 100 ml of dehydrated acetonitrile and reaction mixture was refluxed for 24 h under nitrogen. After completion of the reaction, solvent was evaporated and the crude product was washed with ample diethyl ether giving 5.7 g of titled compound as whitish powder in 91% yield having 99% purity as confirmed by HPLC. FAB-mass (measured 188.0; calculated 188.13).

*2.2.6. Synthesis of 3-butoxy-4-[(1-ethyl-1,3-dihydro-3,3-dimethyl-2H-indole-2-ylidene)methyl]-3-cyclobutene-1,2-dione [**8**]*

In a round bottom flask fitted with condenser, 1.26 g (4 mmol) of [**7**], 900 mg (4 mmol) of 3,4-dibutoxy-3-cyclobutene-1,2-dione, 0.8 ml of triethylamine were dissolved in 6 ml butanol. Reaction mixture was heated at 70 °C for 1 h leading to green solution. Solvent was removed at rotary evaporator and product was purified by column chromatography (silica gel) with ethyl acetate and hexane as eluent giving 920 mg of titled compound in 50% yield and 99% purity as confirmed by HPLC. Compound was confirmed by MALDI-TOF-mass [calculated 339.18 and measured 340.60 (M+H)].

2.2.7. Synthesis of squaraine dyes

Symmetrical squaraine dyes **SQ-1**, **SQ-2**, **SQ-3** and **SQ-5** were synthesized using corresponding trimethyl-indolium iodide salt (1 equiv.) and squaric acid (0.5 equiv.) in 1-butanol:toluene mixture (1:1, v/v). Reaction mixture was refluxed for 18 h using Dean-Stark trap. After completion of reaction, reaction mixture was cooled, solvent was evaporated and product was purified by silica gel column chromatography using chloroform:methanol as eluting solvent. Only in the case of **SQ-2** bearing carboxylic acid in substituted alkyl chain, product was confirmed as butyl ester of the dye which was then hydrolyzed to get the free acid. **SQ-2** ester: yield 42%, purity 98%, FAB-mass (calculated 652.25 and observed 652.0). For NMR chart of **SQ-2** ester see Fig. S7. **SQ-1**, yield 39%, purity 98%, MALDI-TOF-mass (calculated 484.16 and observed 484.21) (see Fig. S6 for NMR). **SQ-2**, yield 58%, purity 98%, MALDI-TOF-mass (calculated 540.22 and observed 541.49 (M+H)). **SQ-3**, yield 58%, purity 98%, MALDI-TOF-mass (calculated 540.22 and observed 541.49 (M+H)) see Fig. S8 for NMR. **SQ-5**, yield 46%, purity 97%, MALDI-TOF-mass (calculated 708.41 and observed 708.48 (M+H)) for NMR see Fig. S10.

Unsymmetrical squaraine dye **SQ-4** was synthesized using semi-squaraine ester (**8**) and compound (**2b**) as follows: in a round bottom flask fitted with condenser, 466 mg (1 mmol) of compound (**8**) was dissolved in 10 ml ethanol followed by 0.54 ml (1.5 mmol) of aqueous NaOH. Reaction mixture was refluxed for 30 min which was then cooled followed by addition of 1N HCl (3.6 ml) giving compound (**9**). Solvent was then removed at rotary evaporator followed by addition of 359 mg (1 mmol) of compound (**2b**) and 20 ml of 1-butanol:toluene mixture (1:1, v/v). Reaction mixture was refluxed for 18 h using Dean-Stark trap. Reaction mixture was cooled, solvent was evaporated and product was purified by silica gel column chromatography using chloroform:methanol as eluting solvent. 350 mg of final titled compound was obtained as blue solid in 97% purity as confirmed by HPLC in 64% yield. MALDI-TOF-mass (calculated 497.24 and observed 497.76) confirms the successful synthesis of the unsymmetrical dye **SQ-4**. For NMR chart and analysis see Fig. S9.

2.3. DSSC fabrication and measurement of cell performance

DSSC were fabricated using Ti-Nanoxide D paste (Solaronix SA) which was coated on a Low E glass (Nippon Sheet Glass Co., Ltd.) by a doctor blade. The substrate was then baked at 450 °C to fabricate TiO_2 layers of about 12 μm thickness. The substrate was dipped in the solution containing dye in the presence and/or absence of CDCA. The dye concentration was fixed to be 0.25 mM while CDCA concentration was 2.5 mM. A Pt sputtered SnO_2/F layered glass substrate was employed as the counter electrode. Electrolyte (WWS30) containing LiI (500 mM), iodine (50 mM), *t*-butylpyridine (580 mM), MeEtIm-DCA (ethylmethylimidazolium dicyanoimide) (4:6, wt/wt) (600 mM) in acetonitrile, was used to fabricate the DSSC. A Himilan film (Mitsui-DuPont Polychemical Co., Ltd.) of 25 μm thickness was used as a spacer. The cell area was 0.25 cm^2. Solar cells were evaluated using a photo-mask on the solar cell in order to remove the effect of the optical reflection under the irradiation of 100 mW/cm^2 at AM 1.5.

3. Results and discussion

3.1. Effect of substituents in sensitizing dyes on DSSC performance

Fig. 1 exhibits the photovoltaic performance of DSSC based on symmetrical squaraine dyes being used as sensitizer for nanoporous TiO_2 electrodes. Linking of the dye through the anchoring group to the TiO_2 surface is one of the important requirements for facile electron injection from photoexcited dye to the conduction band of TiO_2. As clearly evident from this figure that **SQ-2** having anchoring functional group –COOH in alkyl side chain substituted at N-position shows the lowest photoconversion efficiency as compared to **SQ-1** and **SQ-3** bearing carboxylic acid functionality directly substituted in the indole ring. It has been widely reported that delocalization and diversion of electron density of LUMO towards the anchoring group leads to facile photo induced electron transfer from the dye to TiO_2 electrode which ultimately results in the improved conversion efficiency [22,23]. In order to have more in depth insight about the photo physical properties of these sensitizers, TD-DFT calculations were performed using B3LYP functional and 6-311g basis set as implemented in G03 program package. The calculated MO picture as shown in Supporting

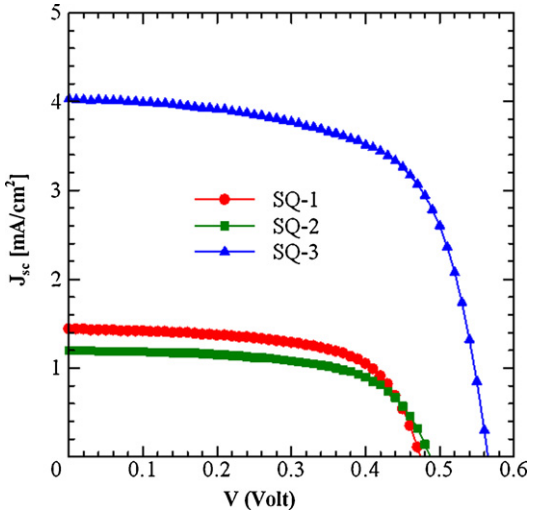

Fig. 1. Photovoltaic performance symmetrical squaraine dyes **SQ-1**, **SQ-2** and **SQ-3** under 100 mA/cm^2 simulated solar irradiation at AM 1.5.

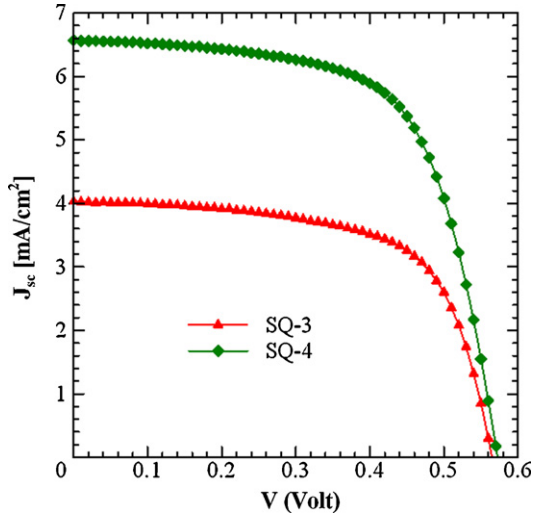

Fig. 3. Effect of molecular asymmetry on the photovoltaic performance of symmetrical (**SQ-3**) and unsymmetrical (**SQ-4**) squaraine dye based on DSSC.

informations (S1 and S2) clearly corroborates that HOMO is mainly delocalized over central squaric acid core while electronic orbital delocalization patterns are different for **SQ-2** as compared to **SQ-1** and **SQ-3**. LUMO is distinctively delocalized over carboxylic functionality in the case of both of the **SQ-1** and **SQ-3**, which is absent in the **SQ-2**. Probably this could be responsible for the inefficient electron transfer from excited dye to TiO_2 leading to decreased conversion efficiency. Similar kind of low conversion efficiency for sensitizers having alkyl side chain carboxyl functionalized sensitizers have also been observed by Matsui et al. [24] and Li et al. [25].

Photo action spectra of DSSC along with the solution phase UV–visible absorption spectra of sensitizers **SQ-1**, **SQ-2** and **SQ-3** have been shown in Fig. 2. Action spectra are symbatic with the absorption spectra with spectral broadening due to aggregate formation in solid state. Action spectra of **SQ-1** and **SQ-3** differ only in the presence and absence of alkyl substituent at N-position of indole ring and introduction of alkyl group leads to enhanced conversion efficiency for **SQ-3** as compared to that of **SQ-1**. Organic dyes with extended π-conjugation like phthalocyanine and squaraines are well known for the aggregate formation and derivatives of cholic acid have been found to break such aggregates leading to enhanced efficiency [26,27]. It is interesting to note

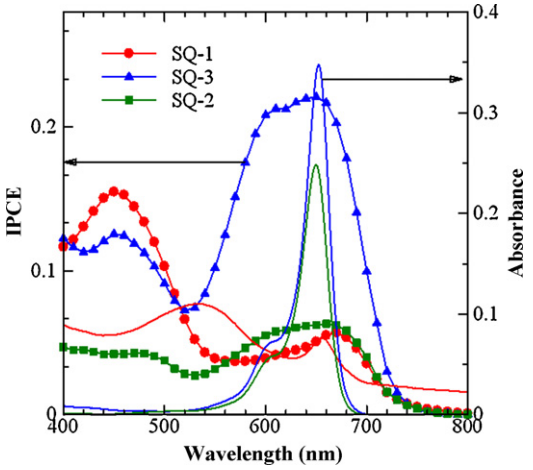

Fig. 2. IPCE curves for DSSC fabricated with **SQ-1**, **SQ-2** and **SQ-3** (lines with symbol) and electronic absorption spectra of these sensitizers in DMF solution (thin line).

that **SQ-1** exhibits a pronounced absorption in lower wavelength region even in solution state which has also been well reflected in the action spectrum. This could be attributed to the formation blue shifted H-aggregates in the solid state upon adsorption of dyes on nanoporous TiO_2. Kim et al. [28] have also emphasized that some squaraine surfactants easily form blue shifted H-aggregates on SnO_2 surfaces absorbing around 500 nm wavelength region. It has also been reported that squaraine dyes are prone to easily form H-aggregates and such aggregates result into the decreased sensitization efficiency of DSSCs [29]. Therefore, such H-aggregates in case of **SQ-1** could be attributed to the decreased efficiency as compared to **SQ-3** where the presence of ethyl group hinders them to some extent leading to relatively enhanced IPCE in higher wavelength region (500–700 nm).

3.2. Effect of asymmetry of dyes on DSSC performance

To study the role of dye asymmetry on photoconversion efficiency, we designed **SQ-3** and **SQ-4** having carboxylic anchoring group directly attached to aromatic ring. Current–voltage (*I–V*) characteristics of DSSC based on these sensitizers under standard global AM 1.5 solar irradiation have been shown in Fig. 3. A perusal of this figure and Table 1 showing photovoltaic parameters clearly indicates that unsymmetrical dye **SQ-4** shows enhanced power conversion efficiency (2.43%) as compared to its symmetrical dye counterpart **SQ-3** (1.46%). It is also interesting to note that the main factor for efficiency enhancement is short circuit current density (J_{sc}) since other cell parameters are nearly the same. Yum et al. [30] have also emphasized that unidirectional flow of electrons from sensitizer to semiconductor surface is responsible for efficient electron transfer from photo excited dye to TiO_2 conduction band.

Table 1
Current–voltage characteristics for DSSC fabricated with various squaraine dyes under 100 mA/cm^2 simulated solar irradiation at global 1.5 condition.

Dye	V_{oc} (V)	J_{sc} (mA/cm^2)	FF	Efficiency (%)
SQ-1	0.47	1.44	0.63	0.43
SQ-2	0.49	1.20	0.62	0.36
SQ-3	0.56	4.03	0.64	1.46
SQ-4	0.57	6.57	0.65	2.43
SQ-5	0.60	5.09	0.69	2.09
SQ-2_DCA	0.55	2.03	0.68	0.76
SQ-3_DCA	0.62	5.79	0.69	2.49
SQ-5_DCA	0.64	7.26	0.68	3.15

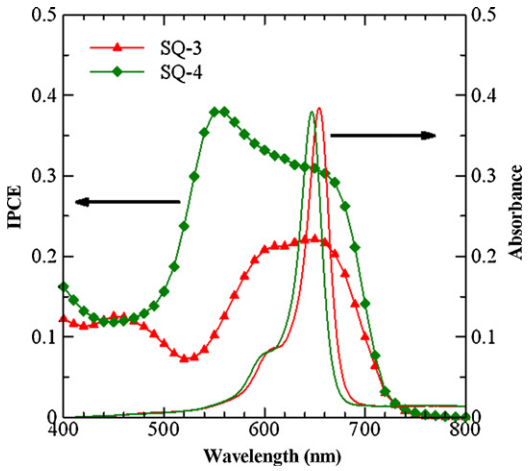

Fig. 4. IPCE curves for DSSC fabricated with **SQ-3**, and **SQ-4** (lines with symbol) and electronic absorption spectra of these sensitizers in DMF solution (thin line).

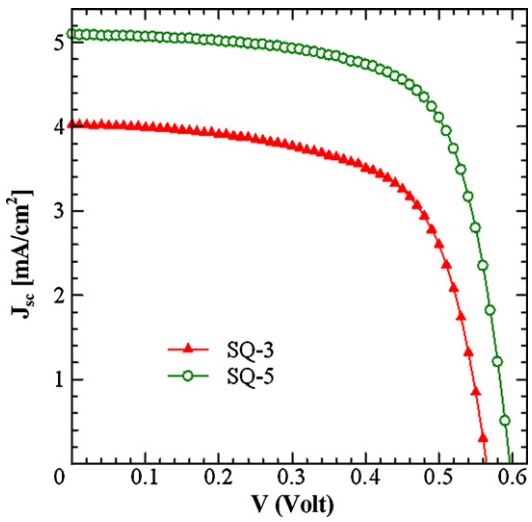

Fig. 5. Photovoltaic performance symmetrical squaraine dye bearing shorter (**SQ-3**) and longer (**SQ-5**) alkyl substituent under 100 mA/cm^2 simulated solar irradiation at AM 1.5.

Therefore, it seems that unsymmetrical dye **SQ-4** provides such a more effective electron transfer environment as compared to that of symmetrical **SQ-3** leading to enhanced J_{sc}.

Photocurrent action spectra DSSC along with UV–visible electronic absorption spectra of **SQ-3** and **SQ-4** in DMF solution is shown in Fig. 4. It clearly shows that although these sensitizers are very similar in electronic absorption but there is a marked improvement in incident monochromatic photon-to-electron conversion efficiency (IPCE) for unsymmetrical sensitizer **SQ-4** as compared to **SQ-3** which could be attributed to the enhanced overall power conversion efficiency as shown in Fig. 3. A key requirement for the facile electron transfer is a good electronic coupling between LUMO of the dye and TiO_2 conduction band which can be obtained by strong electronic conjugation between sensitizer core and anchoring group. Structure of **SQ-2** as shown in Scheme 1 indicates that the lack of such conjugation between dye core and anchoring group could be responsible for the very small conversion efficiency provided by this sensitizer. Both of sensitizers, **SQ-3** and **SQ-4** meet with this requirement leading to enhanced efficiency as compared to **SQ-2**. TD-DFT calculated MO pictures (see S3 and S4 in Supporting information) show distinctively different electron density distribution for **SQ-3** and **SQ-4**. LUMO picture for unsymmetrical **SQ-4** show a clear unidirectional shift of electron density from the opposite end of the molecule towards the anchoring carboxylic acid group which is bidirectional for the symmetrical dye **SQ-3**. Such a unidirectional flow of electron density is expected for favorable charge separation and facile electron injection [30,31].

3.3. *Effect of alkyl chain length on DSSC performance*

A perusal of the photovoltaic performance of DSSC based on squaraine dyes as shown in Fig. 5 and Table 1 clearly corroborates that enhanced conversion efficiency was observed for the SQ-dye having the long alkyl chain length. This increase in efficiency was associated with the increase in both of the V_{oc} as well as J_{sc}. Koumura et al. have also advocated the importance of the presence of longer alkyl chain in their MK dyes towards efficiency enhancement [32]. Enhancement of the V_{oc} as function of alkyl chain length in these squaraine dyes was elucidated by dark *I–V* characteristics. Shift of onset of the dark currents towards higher voltage indicates the suppression of recombination leading to improved V_{oc} for squaraine bearing longer alkyl chains. Recently, Sakaguchi et al. [27] have reported the increase in the V_{oc} with the increase in surface potential for different sensitizer, which was reasoned with the upward shift of the conduction band edge of TiO_2. Based on surface potential measurement using Kelvin-probe method, Pandey et al. [33] have reported that the surface potential of squaraine dyes was also found to increase with the increasing alkyl chain length and could, therefore, be attributed to the increase in V_{oc}.

Enhancement of J_{sc} was elucidated with IPCE measurement after DSSC fabrication as shown in Fig. 6 and the extent of dye adsorption on the TiO_2 surface. As clearly evident from Fig. 6 that there is spectral broadening of IPCE along with the increase of its magnitude could be attributed to the enhanced J_{sc} for the **SQ-5** having the relatively longer alkyl substituent. Recently, Ogomi et al. [34] have demonstrated that increase in the extent of adsorbed dyes on TiO_2 surface leads to enhanced surface trap passivation leading to increased J_{sc}. It is interesting to note that the extent of the dye adsorbed on TiO_2 surface was found to be larger (16 nmol cm^{-2} μm^{-1}) for **SQ-5** as compared to that of **SQ-3** (10 nmol cm^{-2} μm^{-1}) which supports the increased J_{sc} for squaraine dyes having longer alkyl chain length due to the enhanced TiO_2 surface trap passivation.

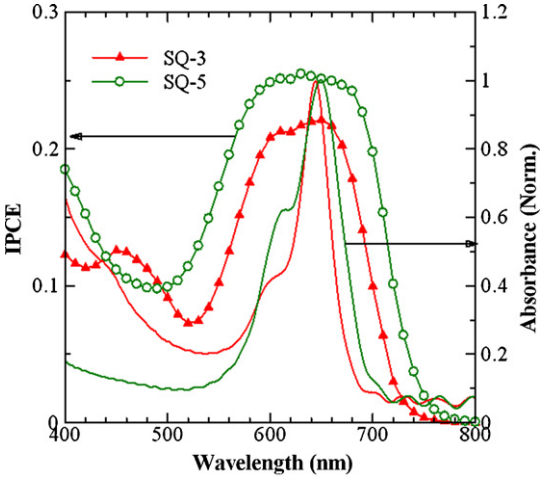

Fig. 6. Photo action spectra for DSSC fabricated with **SQ-3** (filled triangle) and **SQ-5** (open circle) and electronic absorption spectra (thin line) of these sensitizers in DMF solution.

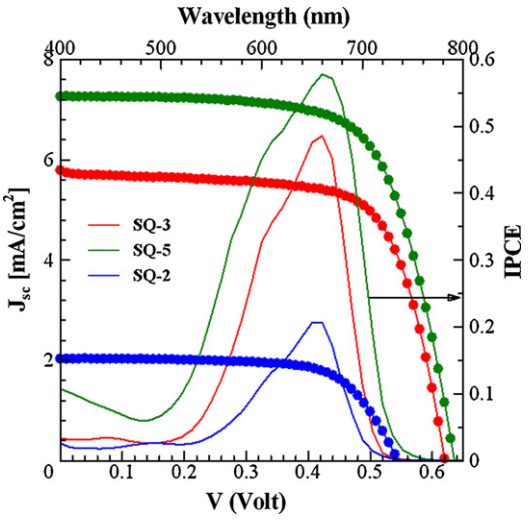

Fig. 7. Photovoltaic performances (line with symbol) and action spectra of (thin line) for symmetrical squaraine dyes **SQ-2**, **SQ-3** and **SQ-5** after DSSC fabrication in the presence of CDCA under 100 mA/cm^2 simulated solar irradiation at AM 1.5.

3.4. Effect of chenodeoxycholic acid as co-adsorbent on DSSC performance

A number of cholic acid derivatives have been frequently employed as co-adsorbent along with sensitizing dyes for the enhancement of efficiency of DSSC [35]. Using various cyanine dyes Sayama et al. [36] have advocated that use of cholic acid as co-adsorbent along with sensitizing dye leads to the decrease in the leakage current attributed to the enhancement of their DSSC efficiency. Kopidakis et al. [37] emphasized that incorporation of CDCA is associated with upward shift of TiO_2 conduction band edge leading to enhancement of V_{oc} and thus DSSC performance based on their transient photovoltage measurements. *I–V* characteristics and DSSC efficiency parameters shown in Fig. 7 and Table 1, respectively, clearly indicates that introduction of CDCA as co-adsorbent leads to the enhancement of the over all cell efficiency by increasing both the V_{oc} and J_{sc} in the case of the all of the organic SQ-dyes under investigation as compared to DSSC fabricated using these dyes in the absence of CDCA. A similar observation has also been made by Wang et al. [38] where both of J_{sc} and V_{oc} were found to be increased upon increasing the CDCA concentration in the case of their coumarin based organic dyes.

A careful perusal of *I–V* characteristics corroborates that although both V_{oc} and J_{sc} are getting improved upon introduction of CDCA in the case of the SQ-dyes but improvement in the J_{sc} is much pronounced for the dyes **SQ-3** and **SQ-5** having anchoring –COOH group directly substituted in the aromatic ring as compared to that of **SQ-2** bearing side chain substituted carboxylic acid anchoring moiety. This could be attributed to the efficient electron injection from photoexcited **SQ-5** and **SQ-3** as compared to **SQ-2** to the TiO_2 conduction band due to conjugation of COOH electron density to the aromatic ring. Yum et al. [30] have also emphasized that a strong conjugation across the chromophoric main body and the anchoring group is highly required for a good electronic coupling between the LUMO of the dye and TiO_2 conduction band. It is interesting to note that lack of electron density on the LUMO of carboxylic acid anchoring group in **SQ-2** could be attributed to its decreased photosensitization behavior as compared SQ-dyes having ring substituted –COOH group bearing sufficient electron density at the anchoring group. Another role of CDCA has been reported to suppress the dye aggregation resulting into the suppression of charge recombination between the injected electrons and I_3^- ions of the electrolyte. Khazraji et al. have also emphasized that as compared to the dye aggregates, monomers can inject electrons to TiO_2 more efficiently [39]. A perusal of dye structures of SQ-dyes as shown in Scheme 1 clearly indicates that **SQ-3** having shorter alkyl substituent (ethyl) is relatively prone to form π-stacked dye aggregates as compared to that **SQ-5** where the long alkyl chain (octyl) resist the easy dye aggregation. In the presence of CDCA these π-stacked aggregates get broken leading to facile electron injection yield and thus J_{sc}.

A perusal of action spectrum as shown in Fig. 6 (solid line) clearly indicates that there is a clear enhancement of IPCE maximum upon the introduction of CDCA for the dyes **SQ-2**, **SQ-3** and **SQ-5** as compared to IPCE for these dyes in the absence of CDCA as shown in Figs. 2 and 6, which could be attributed enhanced J_{sc}. Following the similar trend as observed in the *I–V* characteristics, there was an enhancement of IPCE for **SQ-2** (6–21%), **SQ-3** (22–49%) and **SQ-5** (25–58%) in the presence of CDCA at 660 nm. The increased IPCE for **SQ-2** even after DCA introduction was much smaller as compared to the **SQ-3** and **SQ-5** indicates that in spite of π-aggregation diminished electron injection from excited dye molecule to TiO_2 conduction band could be attributed to be responsible for its lower photoconversion efficiency.

4. Conclusion

Squaraine core based novel organic sensitizers have been synthesized and their sensitization behaviour has been evaluated by fabricating the DSSC. Various factors such as position of anchoring group, molecular asymmetry, effect of alkyl chain length and dye aggregation on sensitization behaviour have been addressed. It has been demonstrated that attachment of anchoring group in the aromatic ring and creation of molecular asymmetry facilitates the effective electron injection from photoexcited dye molecule to the conduction band of TiO_2 leading to enhanced photovoltaic performance. Even in the absence of CDCA unsymmetrical dye **SQ-4** shows nearly double conversion efficiency (2.43%) as compared to its symmetrical dye counterpart **SQ-3** (1.46%) having similar alkyl chain length. Long alkyl chain substitution in the squaraine sensitizers not only leads to suppression of dye aggregation but also leads to better TiO_2 surface passivation resulting in to enhanced V_{oc} and J_{sc} after DSSC fabrication.

Acknowledgement

Authors would like to acknowledge the financial support from the New Energy Industrial Technology Development Organization (NEDO), Japan.

Appendix A. Supplementary data

Supplementary data associated with this article can be found, in the online version, at doi:10.1016/j.jphotochem.2010.04.015.

References

[1] M. Gratzel, Solar energy conversion by dye-sensitized photovoltaic cells, Inorg. Chem. 44 (2005) 6841–6851.
[2] M.K. Nazeeruddin, F. De Angelis, S. Fantacci, A. Selloni, G. Viscardi, P. Liska, S. Ito, B. Takeru, M. Gratzel, Combined experimental and DFT–TDDFT computational study of photoelectrochemical cell ruthenium sensitizers, J. Am. Chem. Soc. 127 (2005) 16835–16847.
[3] G.L. Zhang, H. Bala, Y.M. Cheng, D. Shi, X.J. Li, Q.J. Yu, P. Wang, High efficiency and stable dye-sensitized solar cells with an organic chromophore featuring a binary π-conjugated spacer, Chem. Commun. (2009) 2198–2200.
[4] S. Ito, H. Miura, S. Uchida, M. Takata, K. Sumioka, P. Liska, P. Comte, P. Pechy, M. Gratzel, High-conversion-efficiency organic dye-sensitized solar cells with a novel indoline dye, Chem. Commun. (2008) 5194– 5196.
[5] W.M. Campbell, K.W. Jolley, P. Wagner, K. Wagner, P.J. Walsh, K.C. Gordon, L. Schmidt-Mende, M.K. Nazeeruddin, Q. Wang, M. Gratzel, D.L. Officer, Highly

efficient porphyrin sensitizers for dye-sensitized solar cells, J. Phys. Chem. C 111 (2007) 11760–11762.
[6] K. Takechi, P.V. Kamat, R.R. Avirah, K. Jyothish, D. Ramaiah, Harvesting infrared photons with croconate dyes, Chem. Mater. 20 (2008) 265–272.
[7] P.Y. Reddy, L. Giribabu, C. Lyness, H.J. Snaith, C. Vijaykumar, M. Chandrasekharam, M. Lakshmikantam, J.H. Yum, K. Kalyanasundaram, M. Gratzel, M.K. Nazeeruddin, Efficient sensitization of nanocrystalline TiO_2 films by a near-IR absorbing unsymmetrical zinc phthalocyanine, Angew. Chem. Int. Ed. 46 (2007) 373–376.
[8] W. Zhao, Y.J. Hou, X.S. Wang, B.W. Zhang, Y. Cao, R. Yang, W.B. Wang, X.R. Xiao, Study on squarylium cyanine dyes for photoelectric conversion, Sol. Energy Mater. Sol. Cells 58 (1999) 173–183.
[9] L. Giribabu, C.V. Kumar, V.G. Reddy, P.Y. Reddy, C.S. Rao, S.R. Jang, J.H. Yum, M.K. Nazeeruddin, M. Gratzel, Unsymmetrical alkoxy zinc phthalocyanine for sensitization of nanocrystalline TiO_2 films, Sol. Energy Mater. Sol. Cells 91 (2007) 1611–1617.
[10] F. Inakazu, Y. Noma, Y. Ogomi, S. Hayase, Dye-sensitized solar cells consisting of dye-bilayer structure stained with two dyes for harvesting light of wide range of wavelength, Appl. Phys. Lett. 93 (2008) 93304.
[11] Y.S. Chen, Z.H. Zeng, C. Li, W.B. Wang, X.S. Wang, B.W. Zhang, Highly efficient co-sensitization of nanocrystalline TiO_2 electrodes with plural organic dyes, New J. Chem. 29 (2005) 773–776.
[12] Y. Noma, K. Iizuka, Y. Ogomi, S.S. Pandey, S. Hayase, Preparation of double dye-layer structure of dye-sensitized solar cells from cocktail solutions for harvesting light in wide range of wavelengths, Jpn. J. Appl. Phys. 48 (2009) 020213.
[13] K.Y. Law, F.C. Bailey, Squarine chemistry – synthesis, characterization and optical properties of a class of novel unsymmetrical squarines 4-(dimethylamino)-phenyl(4′-methoxyphenyl)-squarine and its derivatives, J. Org. Chem. 57 (1992) 3278–3286.
[14] K.Y. Law, Organic photoconductive materials – recent trends and developments, Chem. Rev. 93 (1993) 449–486.
[15] A. Otsuka, K. Funabiki, N. Sugiyama, T. Yoshida, Dye sensitization of ZnO by unsymmetrical squaraine dyes suppressing aggregation, Chem. Lett. 35 (2006) 666–667.
[16] S. Alex, U. Santhosh, S. Das, Dye sensitization of nanocrystalline TiO_2: enhanced efficiency of unsymmetrical versus symmetrical squaraine dyes, J. Photochem. Photobiol. A 172 (2005) 63–71.
[17] A. Mishra, R.K. Behera, P.K. Behera, B.K. Mishra, G.B. Behera, Cyanines during the 1990s: a review, Chem. Rev. 100 (2000) 1973–2011.
[18] A. Mishra, M.K.R. Fischer, P. Bauerle, Metal-free organic dyes for dye-sensitized solar cells: from structure, property relationships to design rules, Angew. Chem. Int. Ed. 48 (2009) 2474–2499.
[19] X. Chen, X. Peng, A. Cui, B. Wang, L. Wang, R. Wang, Photostabilities of novel heptamethine 3H-indolenine cyanine dyes with different *N*-substituents, J. Photochem. Photobiol. A 181 (2006) 79–85.
[20] W. Pham, W.F. Lai, R. Weissleder, C.H. Tung, High efficiency synthesis of a bioconjugatable near-infrared fluorochrome, Bioconjugate Chem. 14 (2003) 1048–1051.
[21] B. Oswald, L. Patsenker, J. Duschl, H. Szmacinski, O.S. Wolfbeis, E. Terpetschnig, Synthesis, spectral properties, and detection limits of reactive squaraine dyes, a new class of diode laser compatible fluorescent protein labels, Bioconjugate Chem. 10 (1999) 925–931.
[22] C. Kim, H. Choi, S. Kim, C. Baik, K. Song, M.S. Kang, S.O. Kang, J. Ko, Molecular engineering of organic sensitizers containing *p*-phenylene vinylene unit for dye-sensitized solar cells, J. Org. Chem. 73 (2008) 7072–7079.
[23] D.P. Hagberg, T. Marinado, K.M. Karlsson, K. Nomura, P. Qin, G. Boschloo, T. Brinck, A. Hagfeldt, L. Sun, Tuning the HOMO and LUMO energy levels of organic chromophores for dye sensitized solar cells, J. Org. Chem. 72 (2007) 9550–9556.
[24] M. Matsui, Y. Hashimoto, K. Funabiki, J.Y. Jin, T. Yoshida, H. Minoura, Application of near-infrared absorbing heptamethine cyanine dyes as sensitizers for zinc oxide solar cell, Synth. Met. 148 (2005) 147–153.
[25] C. Li, W. Wang, X.S. Wang, B.W. Zhang, Y. Cao, Molecular design of squaraine dyes for efficient far-red and near-IR sensitization of solar cells, Chem. Lett. 34 (2005) 554–555.
[26] M.K. Nazeeruddin, R. Humphry-Baker, M. Gratzel, D. Wohrle, G. Schnurpfeil, G. Schneider, A. Hirth, N. Trombach, Efficient near-IR sensitization of nanocrystalline TiO2 films by zinc and aluminum phthalocyanines, J. Porphyrins Phthalocyanines 3 (1999) 230–237.
[27] S. Sakaguchi, S.S. Pandey, K. Okada, Y. Yamaguchi, S. Hayase, Probing TiO_2/dye interface in dye sensitized solar cells using surface potential measurement, Appl. Phys. Exp. 1 (2008) 105001.
[28] Y.S. Kim, K.N. Liang, K.Y. Law, D.G. Whitten, An investigation of photocurrent generation by squarine aggregates in monolayer modifies SnO_2 electrodes, J. Phys. Chem. 98 (1994) 984–988.
[29] Z.S. Wang, K. Hara, Y. Dan-Oh, C. Kasada, A. Shinpo, S. Suga, H. Arakawa, H. Sugihara, Photophysical and (photo)electrochemical properties of a coumarin dye, J. Phys. Chem. B 109 (2005) 3907–3914.
[30] J.H. Yum, P. Walter, S. Huber, D. Rentsch, T. Geiger, F. Nuesch, F. De Angelis, M. Gratzel, M.K. Nazeeruddin, Efficient far-red sensitization of nanocrystalline TiO_2 films by an unsymmetrical squaraine dye, J. Am. Chem. Soc. 129 (2007) 10320–10321.
[31] K. Hara, T. Sato, R. Katoh, A. Furube, Y. Ohga, A. Shinpo, S. Suga, K. Sayama, H. Sugihara, H. Arakawa, Molecular design of coumarin dyes for efficient dye-sensitized solar cells, J. Phys. Chem. B 107 (2003) 597–606.
[32] N. Koumura, Z.S. Wang, S. Mori, M. Miyashita, E. Suzuki, K. Hara, Alkyl-functionalized organic dyes for efficient molecular photovoltaics, J. Am. Chem. Soc. 128 (2006) 14256–14257.
[33] S.S. Pandey, S. Sakaguchi, Y. Yamaguchi, S. Hayase, Influence of nature of surface dipoles on observed photovoltage in dye-sensitized solar cells as probed by surface potential measurement, Org. Electr. 11 (2010) 419–426.
[34] Y. Ogomi, Y. Kashiwa, Y. Noma, Y. Fujita, S. Kojima, M. Kono, Y. Yamaguchi, S. Hayase, Photovoltaic performance of dye-sensitized solar cells stained with black dye under pressurized condition and mechanism for high efficiency, Sol. Energy Mater. Sol. Cells 93 (2009) 1009–1012.
[35] A. Kay, M. Gratzel, Artificial photosynthesis; photosensitization of TiO_2 solar cells with chlorophyll derivatives and related natural porphyrines, J. Phys. Chem. 97 (1993) 6272–6277.
[36] K. Sayama, S. Tsukagoshi, T. Mori, K. Hara, Y. Ohga, A. Shinpou, Y. Abe, S. Suga, H. Arakawa, Efficient sensitization of nanocrystalline TiO_2 films with cyanine and merocyanine organic dyes, Sol. Energy Mater. Sol. Cells 80 (2003) 47–71.
[37] N. Kopidakis, N.R. Neale, A.J. Frank, Effect of an adsorbent on recombination and band-edge movement in dye-sensitized TiO_2 solar cells: evidence for surface passivation, J. Phys. Chem. B 110 (2006) 12485–12489.
[38] Z.S. Wang, Y. Cui, Y. Dan-Oh, C. Kasada, A. Shinpo, K. Hara, Thiophene-functionalized coumarin dye for efficient dye-sensitized solar cells: electron lifetime improved by coadsorption of deoxycholic acid, J. Phys. Chem. C 111 (2007) 7224–7230.
[39] A.C. Khazraji, S. Hotchandani, S. Das, P.V. Kamat, Controlling dye (merocyanine-540) aggregation on nanostructured TiO_2 films: an organized assembly approach for enhancing the efficiency of photosensitization, J. Phys. Chem. B 103 (1999) 4693–4700.